

Hot and Dense Hadronic Matter - Selected Topics -

Wolfram WEISE

*Physik-Department, Technische Universität München
D-85747 Garching, Germany*

Recent developments in the area of hadronic and quark-gluon matter under extreme conditions are surveyed. A prime topic is the possible interplay of chiral and deconfinement transitions in QCD. The symmetry breaking pattern of QCD features two seemingly disconnected phenomena: the spontaneous breakdown of the $Z(3)$ center symmetry in the deconfinement transition of pure-gauge QCD, and the spontaneous breaking of chiral $SU(N_f) \times SU(N_f)$ symmetry in the limit of N_f massless quark flavors. The dynamical entanglement of these symmetries is discussed in the framework of a schematic model (the PNJL model) in comparison with results from lattice QCD. The QCD phase diagram is also explored from this viewpoint, with emphasis on the (uncertain) location of the critical point. Aspects of compressed baryonic matter at zero temperature and its nuclear physics connection are sketched in view of new results for the density dependence of the chiral condensate.

§1. Matter produced at RHIC: keywords

The fireball produced at RHIC in the PHENIX and STAR experiments¹⁾ has featured several unexpected phenomena. Transverse energy yields, jet quenching, flow anisotropy and its analysis in terms of hydrodynamics, all lead to the following conclusions:

- the initial energy densities reached are as large as $\mathcal{E} \sim 10 - 20 \text{ GeV fm}^{-3}$;
- the quark-gluon matter is strongly coupled and opaque;
- its properties are reminiscent of a nearly perfect fluid.

Equilibration appears to proceed extremely fast. The subsequent hadronization and systematics of particle production at chemical freezeout can be given a simple interpretation:²⁾ a thermal (grand canonical) description of hadron yields works surprisingly well. These observations are successfully parametrized in terms of a limiting temperature at zero baryon chemical potential, $T_{lim} \simeq 160 \text{ MeV}$, which is reached in the heavy-ion collisions for nucleon-nucleon center-of-mass energies $\sqrt{s_{NN}} \gtrsim 10 \text{ GeV}$. Extrapolations of the freeze-out curve to non-zero chemical potential, up to about $\mu_B \sim 0.8 \text{ GeV}$, raise interesting questions about the relationship of these semi-empirical results to the QCD phase boundary in the plane of temperature T and quark chemical potential $\mu = \mu_B/3$. Exploring the QCD phase diagram in all its configurations is thus an objective of prime importance.

§2. Lattice QCD: thermodynamics

Much of our present level of knowledge about QCD phases derives from lattice QCD thermodynamics. An important issue is the interplay between chiral and

deconfinement transitions and their corresponding critical temperature(s) T_c . Of particular interest is the behavior, as function of temperature, of the chiral (quark) condensate and the Polyakov loop. The chiral condensate controls the transition from spontaneously broken chiral symmetry in its Nambu-Goldstone realization at low temperature, to the restoration of chiral symmetry in its Wigner-Weyl realization at high temperature. The Polyakov loop is a measure of the transition from confinement in the low-temperature hadronic phase, to deconfinement in the high-temperature quark-gluon phase.

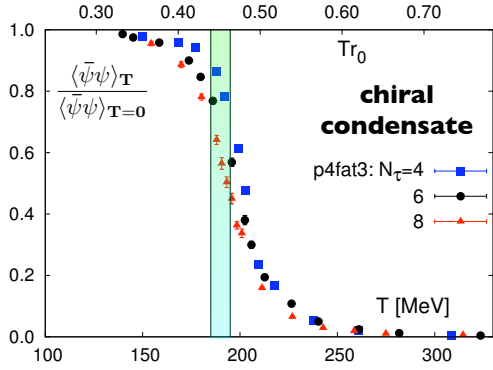


Fig. 1. Temperature dependence of the chiral condensate from lattice QCD with 2 + 1 quark flavours and almost physical quark masses. Adapted from Ref.³⁾

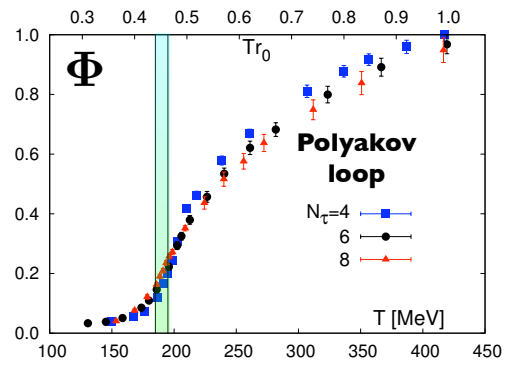


Fig. 2. Temperature dependence of the Polyakov loop from lattice QCD with 2 + 1 quark flavours and almost physical quark masses. Adapted from Ref.³⁾

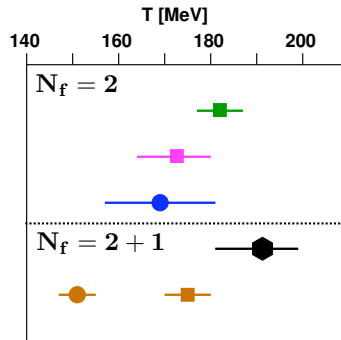


Fig. 3. Transition temperatures for chiral (circular dots) and deconfinement (squares) crossovers from lattice QCD. Results for $N_f = 2$ (upper panel) and $N_f = 2 + 1$ (lower) panel are shown for comparison. The $N_f = 2 + 1$ data are taken from Ref.³⁾ (upper) and Ref.⁵⁾ (lower). Figure adapted from Ref.⁴⁾

Recent updated lattice QCD (LQCD) results for these quantities are shown in Figures 1 and 2. It is established from such LQCD studies that with inclusion of quarks, the chiral and deconfinement transitions are continuous crossovers, so that a critical temperature in the strict sense of a phase transition does not exist. It is nonetheless possible to identify transition temperatures by examining the maxima of

corresponding susceptibilities. Such an analysis³⁾ gives a common transition temperature of about 190 MeV for the case of $N_f = 2+1$ quark flavors with almost physical quark masses: the chiral and deconfinement crossover transitions seem to coincide. However, the situation is still under dispute. Previously obtained lattice results⁵⁾ are at variance with the more recent ones³⁾ as displayed in Fig.3. It is important that this issue be clarified in the near future.

The equation of state of strongly interacting matter is now at hand as a function of temperature T and in a limited range of quark chemical potentials μ . Strategies for circumventing the fermion sign problem characteristic of finite μ are: improved multi-parameter reweighting techniques⁶⁾, Taylor series expansion methods⁷⁾⁻⁹⁾ and analytic continuation from imaginary chemical potential¹⁰⁾⁻¹²⁾. LQCD data exist for the pressure, the energy and entropy densities, quark densities and selected susceptibilities.

§3. Symmetries and symmetry breaking patterns

The two prominent phenomena characteristic of low-energy QCD, confinement and spontaneous chiral symmetry breaking, are governed by basic symmetry principles of QCD in limiting situations:

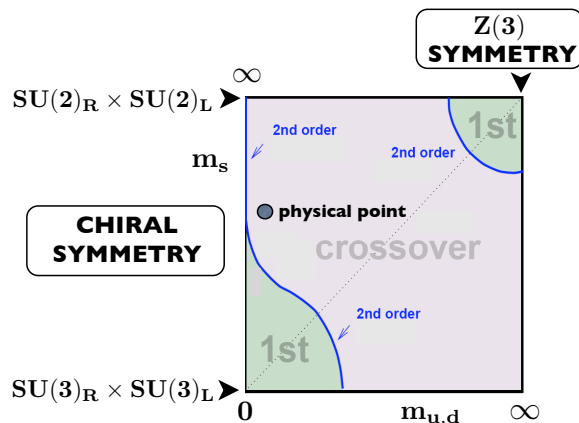


Fig. 4. Expected symmetry breaking pattern of QCD and phase boundaries illustrated in a sketch showing the qualitative dependence on the quark masses $m_{u,d}$ and m_s . Corners represent limiting situations in which exact chiral and $Z(3)$ symmetries are realized. Regions of first order phase transitions are indicated. They are separated from the crossover domain by second order phase transition lines. The physical point with $m_{u,d} \sim 5$ MeV and $m_s \sim 0.1$ GeV is expected to be located in the crossover area. Adapted from Ref.¹⁰⁾.

i) An exact symmetry associated with the center $Z(3)$ of the local $SU(3)$ color gauge group is realized in pure gauge QCD, i.e. for *infinitely heavy* quarks, the limit in which gluons are the only active degrees of freedom. The deconfinement transition in this limiting situation is known to be a 1st order phase transition. In the high-temperature, deconfinement phase of QCD the $Z(3)$ symmetry is spontaneously broken, with the Polyakov loop acting as the order parameter.

ii) Chiral $SU(N_f)_R \times SU(N_f)_L$ symmetry is an exact global symmetry of QCD with N_f massless quark flavors. In the low-temperature (hadronic) phase this symmetry is spontaneously broken down to the flavor group $SU(N_f)_V$ (the isospin group for $N_f = 2$ and the “eightfold way” for $N_f = 3$). As consequence there exist $2N_f + 1$ pseudoscalar Nambu-Goldstone bosons and the QCD vacuum is non-trivial. It hosts quark condensates $\langle \bar{q}q \rangle$ which act as chiral order parameters. In the limit of $N_f = 2$ massless quarks the transition from spontaneously broken chiral symmetry to its restoration in the Wigner-Weyl realization is a 2nd order phase transition signaled by the “melting” of the quark condensate. For $N_f = 3$ massless quarks this phase transition is first order.

These two different symmetry breaking scenarios act in opposite corners of the so-called Columbia plot (see Fig.4). There is no fundamental reason why they should be connected. Confinement of massless quarks implies spontaneous chiral symmetry breaking, whereas the reverse is not necessarily true. Whether and under which conditions the chiral and deconfinement transitions coincide, as apparent in some recent lattice QCD results, is therefore a crucial question.

§4. Modelling the chiral and deconfinement transitions of QCD

This section briefly summarizes a model that combines the two basic principles of low-energy QCD just outlined: confinement and spontaneous chiral symmetry breaking. The confinement aspect is implemented through the dynamics of the Polyakov loop¹³⁾. Chiral symmetry and its spontaneous breakdown at low temperature are the prominent features of the time-honoured schematic model of Nambu and Jona-Lasinio (NJL)^{14),15)}. The synthesis of both approaches is called the PNJL model.

The PNJL model has turned out to be a useful device in order to interpret LQCD results, to understand the thermodynamics around and above T_c in terms of quasiparticles, and to extrapolate into regions not accessible by lattice computations. This model also contributes to the question about the entanglement between chiral and deconfinement transitions. It is designed much in analogy with a Ginzburg-Landau type approach: identifying the relevant order parameters as collective degrees of freedom which govern the dynamics and thermodynamics. Earlier versions of such a model have been discussed in Refs.¹⁶⁾⁻¹⁸⁾. Here we summarize recent results and developments of the two-flavor PNJL model¹⁹⁾⁻²²⁾, including successful comparisons with a variety of LQCD data. For related works see refs.²⁴⁾⁻²⁶⁾.

The two-flavor PNJL model starts from the following Euclidean action:

$$\mathcal{S}(\psi, \psi^\dagger, \phi) = \int_0^{\beta=1/T} d\tau \int_V d^3x \left[\psi^\dagger \partial_\tau \psi + \mathcal{H}(\psi, \psi^\dagger, \phi) \right] + \frac{V}{T} \mathcal{U}(\phi, T) \quad (4.1)$$

with the fermionic Hamiltonian density

$$\mathcal{H} = -i\psi^\dagger (\vec{\alpha} \cdot \vec{\nabla} + \gamma_4 \hat{m}_0 - A_4) \psi + \mathcal{V}(\psi, \psi^\dagger), \quad (4.2)$$

where ψ is the $N_f = 2$ doublet quark field and $\hat{m}_0 = \text{diag}(m_u, m_d)$ is the quark mass matrix. The quarks move in a background color gauge field $A_4 \equiv T\phi = iA_0$, where

$A_0 = \delta_{\mu 0} g \mathcal{A}_a^\mu t^a$ with the $SU(3)_c$ gauge fields \mathcal{A}_a^μ and the generators $t^a = \lambda^a/2$. The matrix valued, constant field ϕ relates to the (traced) Polyakov loop as follows:

$$\Phi = \frac{1}{N_c} \text{Tr} \left[\mathcal{P} \exp \left(i \int_0^\beta d\tau A_4 \right) \right] = \frac{1}{3} \text{Tr} e^{i\phi}, \quad (4.3)$$

In a convenient gauge one can choose a diagonal representation, $\phi = \phi_3 \lambda_3 + \phi_8 \lambda_8$, which specifies $\phi_{3,8}$ as field variables representing the Polyakov loop.

The NJL interaction term $\mathcal{V}(\psi, \psi^\dagger)$ consists of four-fermion couplings acting in quark-antiquark and diquark channels. Their construction is ruled by chiral $SU(2) \times SU(2)$ symmetry. The coupling strength and a momentum cutoff scale are determined by the pion decay constant and the chiral condensate at zero temperature, i.e. by key quantities characteristic of the hadronic phase.

The Polyakov loop effective potential $\mathcal{U}(\phi, T)$ in (4.1) models gluon dynamics in the region around the confinement-deconfinement transition in pure gauge QCD. Its construction is guided by the $Z(3)$ center symmetry (which transforms an element $u \in SU(3)_c$ to $\exp(2\pi i n/3)u$ ($n = 1, 2, 3, \dots$)). The basic building blocks for such a potential are therefore $\Phi^* \Phi$, Φ^3 and Φ^{*3} terms. In Refs.^{20)–22)} the effective potential \mathcal{U} has been designed to properly meet group theoretical constraints, with a logarithmic ansatz guided by the $SU(3)$ Haar measure:

$$\frac{\mathcal{U}(\Phi, \Phi^*, T)}{T^4} = -\frac{1}{2} a(T) \Phi^* \Phi + b(T) \ln \left[1 - 6 \Phi^* \Phi + 4 (\Phi^{*3} + \Phi^3) - 3 (\Phi^* \Phi)^2 \right]. \quad (4.4)$$

The temperature dependent prefactors $a(T)$ and $b(T)$ are adjusted such that the

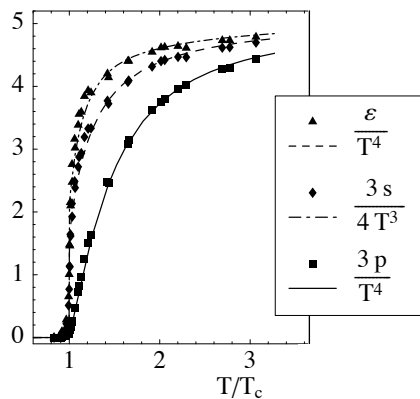


Fig. 5. Scaled energy density ε , entropy density s and pressure p as functions of temperature (given in units of the critical temperature $T_0 = 270$ MeV) of pure gauge QCD. Lattice results²⁷⁾ are compared with the Polyakov loop model (curves)²¹⁾ with parameters as explained in the text.

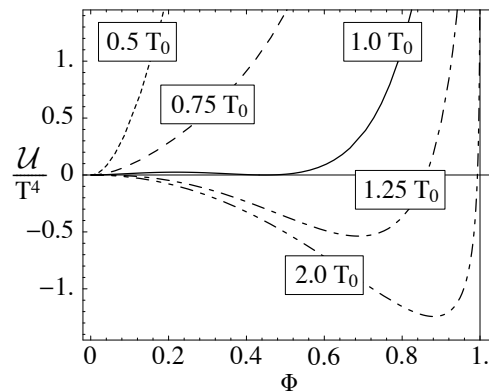


Fig. 6. Effective potential (4.4) for the Polyakov loop Φ at different temperatures (given in units of the critical temperature $T_0 = 270$ MeV) with parameters adjusted to reproduce the pure glue QCD equation of state (see Fig.5).

pressure $p = -\mathcal{U}(T)$ and related thermodynamical quantities reproduce the pure gauge LQCD results for the equation of state with its first order phase transition

at a critical temperature $T_0 \simeq 270$ MeV. Figures 5 and 6 show the resulting fit to the pure gauge QCD equation of state and the Polyakov loop effective potential displaying the first order transition at $T = T_0$.

One can expect such an approach to work at temperatures up to about twice the critical temperature. At much higher temperatures a description of the thermodynamics entirely in terms of the Polyakov loop is no longer adequate as transverse gluons become important. Alternative parametrizations of \mathcal{U} are possible, such as the form guided by strong-coupling considerations¹⁸⁾ which has a different high-temperature limit. These differences are not crucial when considering the transition region, $T \lesssim 2T_c$, where different forms of \mathcal{U} give remarkably similar results as pointed out in Ref.²⁸⁾.

We now proceed to discuss selected applications of PNJL thermodynamics, mostly in comparison with thermal LQCD results. An interesting example is the combination of energy density \mathcal{E} and pressure p known as the “interaction measure”, $\mathcal{E} - 3p$. Results of the PNJL calculation¹⁹⁾ are shown in comparison with earlier two-flavor LQCD data in Fig.7. The impressive improvement of the more recent ($N_f = 2 + 1$) lattice simulations is displayed for comparison in Fig.8.

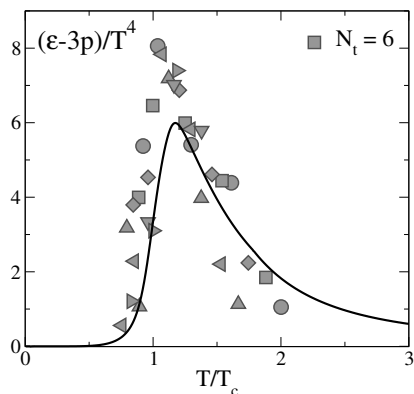


Fig. 7. The “interaction measure”, $\mathcal{E} - 3p$, computed in the PNJL model¹⁹⁾ (solid line) and compared with $N_f = 2$ lattice results from Ref.²⁹⁾

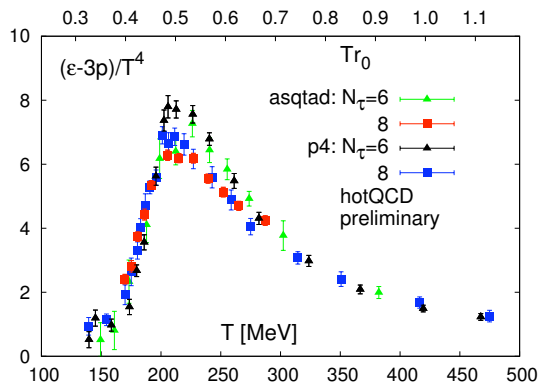


Fig. 8. Update on $N_f = 2 + 1$ lattice QCD data for $\mathcal{E} - 3p$. Taken from Karsch et al.³⁰⁾

A further quantity of interest is the sound velocity c_s given by $c_s^2 = dp/d\mathcal{E}$ at fixed entropy. The PNJL ($N_f = 2$) results for p/\mathcal{E} and c_s^2 (see Fig.9) show the expected characteristically strong T dependence around the critical temperature, in close qualitative correspondence to the behavior seen in the LQCD results for $N_f = 2 + 1$ (see Fig.10).

Perhaps one of the most striking results of the PNJL model is the dynamical entanglement of the chiral and deconfinement crossover transitions. If taken separately, the chiral 2nd order transition in the limit of massless quarks (calculated in the NJL model without implementation of the Polyakov loop) and the 1st order deconfinement transition (as described by the Polyakov loop model without quarks) occur at quite different critical temperatures as shown in Fig. 11. In the PNJL

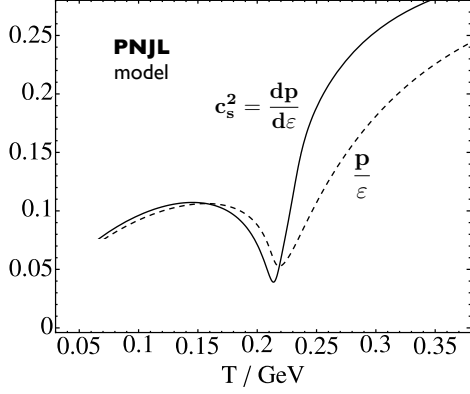


Fig. 9. Ratio p/\mathcal{E} of pressure and energy density and squared sound velocity c_s^2 computed in the PNJL model^{(21), (31)}.

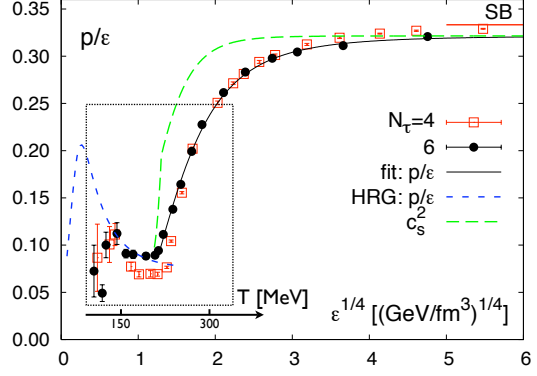


Fig. 10. Ratio p/\mathcal{E} of pressure and energy density deduced from lattice QCD with 2+1 flavors^{(4), (32)}. Solid curve: fit to LQCD data. Short-dashed curve (HRG): hadronic resonance gas estimate. Long-dashed curve: squared sound velocity $c_s^2 = dp/d\mathcal{E}$.

model which couples quark quasiparticles to the Polyakov loop background, chiral symmetry restoration and deconfinement get intertwined in a joint crossover pattern at approximately the same transition temperature. This pattern is shown together with recent lattice results in Fig.12, although this comparison is just meant for general guidance since the LQCD data are generated with 2+1 flavours.

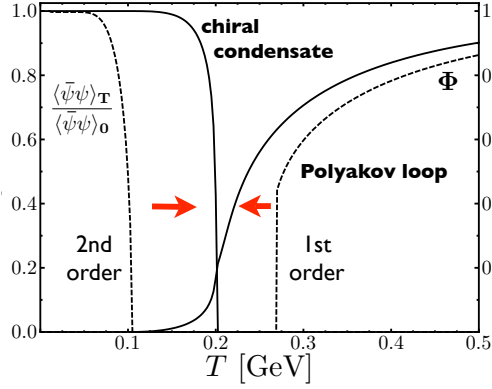


Fig. 11. Left part: chiral condensate normalized to its value at temperature $T = 0$ calculated in the NJL model with $N_f = 2$ massless quarks. Right part: Polyakov loop computed in the pure gauge limit. Solid curves: chiral condensate (with $m_{u,d} = 0$) and Polyakov loop in the PNJL model⁽²¹⁾.

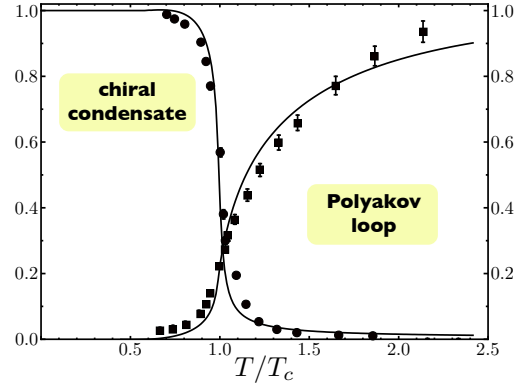


Fig. 12. Chiral condensate (with non-zero quark masses $m_{u,d} = 5$ MeV) and Polyakov loop calculated in the PNJL model^{(21), (36)} showing the joint chiral and deconfinement crossover transitions at $T_c \simeq 200$ MeV. Recent lattice QCD results for $N_f = 2 + 1$ flavours with almost physical masses⁽³⁾ are also shown for orientation.

We finally turn to the phase diagram in the (T, μ) plane as derived^{(22), (31)} from the

two-flavor PNJL model. The result is shown in Fig.13. The solid line represents the crossover transition range between the hadronic phase and the quark-gluon phase. The dashed line marks a first order transition between the phase with spontaneously broken chiral symmetry and the (color) superconducting high-density phase in which diquarks accumulate to form a non-vanishing (Cooper pair) condensate. The transition separating this phase from the quark-gluon sector (marked by the dotted line) is second order. Further inspection²²⁾ reveals that the critical endpoint shown in the figure is not a tricritical point; the three transition lines do not have a common junction. It turns out in fact that the location of this point is extremely sensitive to the input quark mass and to the presence or absence of Polyakov loop dynamics. For example, the temperature at which the gap Δ disappears is shifted upward by about 100 MeV when the Polyakov loop is active, as compared to the standard NJL model. A more detailed discussion can be found in Ref.²²⁾.

The detailed nature of the critical point is still unclear. Extensions of the PNJL model to 2+1 flavours are presently being explored^{28),33)} with inclusion of strange quarks and the axial $U(1)_A$ anomaly. The existence and location of the critical point turns out to be strongly dependent on the coupling parameter of the 'tHooft six-point determinant interaction representing the axial anomaly as derived from instanton dynamics. A global study of $U(1)_A$ breaking mechanisms in both the quark-antiquark and diquark sectors demonstrates³⁴⁾ that, depending on the detailed strengths of the interactions driven by the axial anomaly and on the explicit chiral symmetry breaking by the mass of the strange quark, there may be two critical points, suggesting a smooth crossover at high baryon density from the hadronic to the color-superconducting region. Following the discussion in Ref.³⁵⁾ it cannot even be excluded that there exists no critical point at all in the physically accessible domain. These open issues certainly call for further detailed studies.

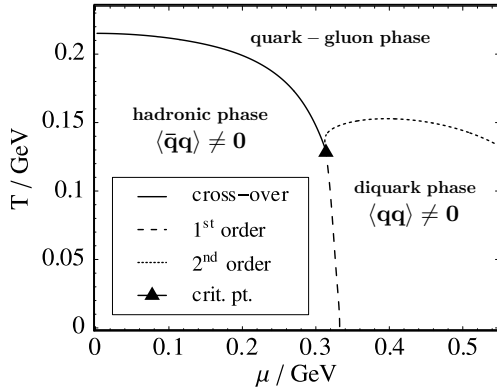


Fig. 13. Phase diagram (in the plane of temperature T versus quark chemical potential μ) computed in the PNJL model²¹⁾ with inclusion of corrections beyond mean-field approximation.³¹⁾

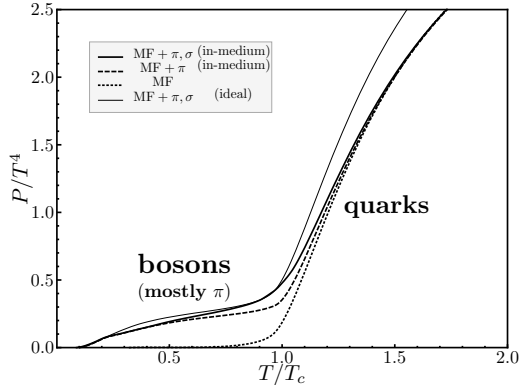


Fig. 14. Pressure as function of temperature at zero chemical potential, calculated in the PNJL model with inclusion of mesonic (quark-antiquark) modes^{31),36)}.

The PNJL model has been extended to include several types of fluctuations

beyond mean field. The most important ones are those involving the leading chiral quark-antiquark modes (pions and scalar-isoscalar fields). The computations are carried out using versions with local and non-local couplings, the latter having the advantage of not introducing the somewhat artificial momentum space cutoff that is characteristic of traditional NJL type models. A typical result (see Fig.14) shows the influence of such mesonic degrees of freedom on the pressure at zero chemical potential. As expected, pions contribute substantially to the pressure below T_c , while at $T > T_c$ quark quasiparticles take over.

§5. From nuclei to compressed baryonic matter

At baryon densities around normal nuclear matter, $\rho_0 \simeq 0.17 \text{ fm}^{-3}$ and beyond, and at low temperatures, the PNJL model does not provide a realistic picture for QCD thermodynamics. The reason is that baryons and their interactions are not properly accounted for. What is really needed in that region is an approach based on chiral pion dynamics including baryons as explicit degrees of freedom. In-medium chiral perturbation theory is such a framework. It works successfully³⁷⁾ in reproducing the nuclear matter equation of state at low temperature and at densities up to about twice ρ_0 . At the same time, when translated into an energy density functional, this theory provides a very satisfactory description for a large variety of empirical properties of nuclei³⁸⁾.

In-medium chiral perturbation theory is the effective field theory constrained by the chiral symmetry breaking pattern of low-energy QCD. It is based on the separation of scales in which the nuclear Fermi momentum p_F , the pion mass m_π and the $\Delta(1230)$ -nucleon mass difference $M_\Delta - M_N \sim 2m_\pi$, are all small compared to the scale characteristic of spontaneous chiral symmetry breaking, $4\pi f_\pi \sim 1 \text{ GeV}$ (with f_π the pion decay constant in vacuum). The active degrees of freedom in this approach are pions coupled to “heavy” baryon sources, the nucleon and the $\Delta(1230)$, with interactions governed by the rules of chiral symmetry. All one- and two-pion exchange processes in the medium are explicitly calculated to three-loop order in the energy density. Short-distance dynamics, not resolved in detail at the Fermi momentum scales under consideration, is encoded in contact interactions with parameters fixed by a few observables.

A question of key importance in the present context is the behavior of the chiral condensate $\langle \bar{\psi}\psi \rangle = \sum_{q=u,d} \langle \bar{q}q \rangle$ as a function of baryon density, at zero temperature. The starting point for this discussion is the QCD Hamiltonian density split into a chiral symmetric part and a quark mass term,

$$\mathcal{H} = \mathcal{H}_0 + \sum_q m_q \bar{q}q . \quad (5.1)$$

Using the Hellmann-Feynman theorem the in-medium chiral condensate is derived as

$$\langle \bar{q}q \rangle_\rho = \left\langle \frac{\partial \mathcal{H}}{\partial m_q} \right\rangle_\rho = \frac{d}{dm_q} \mathcal{E}(p_F)|_{m_q=0} , \quad (5.2)$$

with the energy density \mathcal{E} given as a function of the Fermi momentum p_F . The quark

mass dependence is translated into a dependence on the pion mass m_π through the leading-order Gell-Mann, Oakes, Renner relation in vacuum, $m_\pi^2 = -m_q \langle \bar{\psi}\psi \rangle / f_\pi^2$. Further evaluation gives

$$\frac{\langle \bar{q}q \rangle_\rho}{\langle \bar{q}q \rangle_0} = 1 - \frac{\rho}{f_\pi^2} \left[\frac{\sigma_N}{m_\pi^2} \left(1 - \frac{3p_F^2}{10M_N^2} + \dots \right) + \frac{\partial}{\partial m_\pi^2} \frac{E_{int}(p_F)}{A} \right]. \quad (5.3)$$

The leading linear density dependence of the chiral condensate, corresponding to the limit of a non-interacting Fermi gas of nucleons, is controlled by the sigma term, $\sigma_N = m_q \partial M_N / \partial m_q = 45 \pm 8$ MeV. Non-linear density dependence emerges from the interaction energy per nucleon, E_{int}/A .

In-medium chiral perturbation theory is the proper tool to determine the m_π dependence of the one- and two-pion exchange correlations. Phenomenological boson exchange pictures of the NN interaction are obviously not prepared to handle this problem. The most important contributions come from iterated one-pion exchange and two-pion exchange involving $\Delta(1230)$ excitations, both calculated in the presence of Pauli blocking effects on intermediate nucleon states. The pion exchange tensor force plays a prominent role here, and three-body correlations are naturally incorporated. When all pieces are collected, the resulting density dependence of the chiral condensate in symmetric nuclear matter³⁹⁾ is plotted in Fig.15.

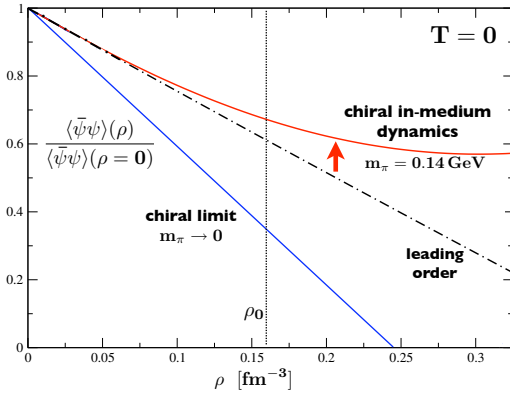


Fig. 15. Chiral condensate in symmetric nuclear matter as function of the baryon density ρ . Dash-dotted curve: leading order linear density dependence (Fermi gas limit). Upper curve: result of in-medium chiral dynamics calculation to three-loop order in the energy density, with physical pion mass. Lower curve: same, but in the chiral limit $m_\pi \rightarrow 0$. Taken from ref.³⁹⁾.

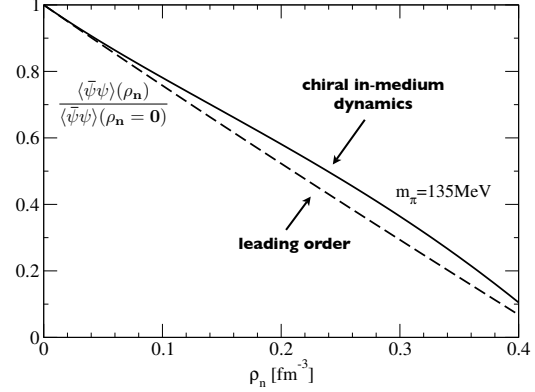


Fig. 16. Chiral condensate in pure neutron matter as function of the neutron density ρ_n . Dashed curve: leading order linear density dependence (Fermi gas limit). Solid curve: result of full in-medium chiral dynamics calculation to three-loop order in the energy density, with physical pion mass. Taken from ref.⁴⁰⁾.

One concludes that two-pion exchange correlations together with the Pauli principle, when taken at the physical value of the pion mass, stabilize the leading linear decrease of the chiral condensate with increasing density. The tendency toward restoration of chiral symmetry is thus delayed and moved to densities far beyond $2\rho_0$. This situation changes drastically in the chiral limit ($m_\pi \rightarrow 0$) as the pion

exchange mechanisms become long-ranged. In this limit chiral restoration would already occur at $\rho \sim 1.5 \rho_0$. Under such conditions, the effective field theory approach based on spontaneous chiral symmetry breaking would not work at typical nuclear densities around ρ_0 . It is an interesting perspective that nuclear physics in its many facets relies so strongly on the up- and down-quark masses being $m_{u,d} \sim 5$ MeV, small but non-zero.

For pure neutron matter, the specific isospin dependence of the relevant two-pion exchange mechanisms just mentioned causes quite a different balance of effects. In this case the corrections to the leading linear density dependence of the chiral condensate turn out to be relatively small⁴⁰⁾ (see Fig.16). In this perspective, the core of neutron stars might be closer to chiral symmetry restoration than compressed nuclear matter with roughly equal number of protons and neutrons. What this means in essence is that the corrections to the scalar mean field arising from correlations in the nuclear medium have both isoscalar and isovector parts which are sizeable individually and about equal in magnitude, with opposite signs. It is of interest to extrapolate such considerations into the regime of exotic nuclei with large proton or neutron excess.

§6. Conclusions and outlook

Exploring the QCD phase diagram with all its complexity is a fundamentally important challenge. Heavy-ion experiments at RHIC give clues about the behavior of matter at extreme initial energy densities and temperatures well beyond the critical temperature scale T_c of about 200 MeV usually associated with the transition from the hadronic to the quark-gluon phase. Hadronic freeze-out, on the other hand, is empirically parametrized in terms of a somewhat lower limiting temperature, $T_{lim} \simeq 160$ MeV. The fact that T_c and T_{lim} do not coincide is not necessarily contradictory, given that - at low baryon chemical potential - the chiral and deconfinement transitions are continuous crossovers rather than phase transitions. Lattice QCD results suggest that the Polyakov loop as an indicator of deconfinement begins its crossover already at temperatures around 150 MeV, well below the critical temperature $T_c \simeq 190$ MeV at which the slope is maximal and the related susceptibility has its peak.

A quasiparticle approach (the PNJL model) encoding the two basic features that govern low-energy QCD, chiral symmetry and confinement, is a useful framework to interpret results from QCD thermodynamics and extrapolate to regions not accessible by lattice computations. It operates with “order parameter” fields, the chiral condensate and the Polyakov loop, coupled through quarks as quasiparticles with dynamically generated masses. Despite its simplicity, this approach turns out to be surprisingly successful in confrontations with lattice data, at least for a temperature range up to about twice the critical temperature $T_c \sim 0.2$ GeV.

Further developments now include extensions beyond mean field theory and the generalisation to 2+1 flavors with inclusion of the axial anomaly, in order to explore the rich structure of the QCD phase diagram. An important step is replacing the notorious NJL cutoff by a running coupling strength and establishing contacts to the

high temperature limit with incorporation of transverse gluons.

Matter at high baryon density leaves much room for further detailed investigations. The existence and location of one or more critical points in the QCD phase diagram is an open issue. It is remarkable that the detailed dynamics related to the axial anomaly in QCD appears to be of qualitative significance in this context. Last not least, the hadronic matter phase with its composite (meson and baryon) degrees of freedom must be approached with an improved effective field theory in order to provide a more realistic equation of state at high baryon density. Advanced in-medium chiral effective field theory calculations of the quark condensate and its density dependence raise new and interesting questions about the role of pion dynamics and isospin in compressed baryonic matter.

Acknowledgements

The author thanks the Yukawa Institute for Theoretical Physics at Kyoto University and in particular Teiji Kunihiro, Kenji Fukushima and Daisuke Jido for their hospitality and for stimulating discussions. Special thanks go to Norbert Kaiser, Thomas Hell, Claudia Ratti and Simon Rössner whose recent works have contributed substantially to the content of this report. This work is partially supported by BMBF, GSI and by the DFG Cluster of Excellence “Origin and Structure of the Universe”.

References

- 1) See reviews at the recent *Quark Matter* conferences.
- 2) A. Andronic, P. Braun-Munzinger and J. Stachel, Nucl. Phys. A **772** (2006), 167.
- 3) M. Cheng et al., Phys. Rev. D **77** (2008), 014511; F. Karsch, arXiv:0711.0661[hep-lat].
- 4) F. Karsch, arXiv:0711.0661[hep-lat].
- 5) Y. Aoki, Z. Fodor, S.D. Katz and K.K. Szabo, Phys. Lett. B **643** (2006), 46.
- 6) Z. Fodor and S.D. Katz, J. High Energy Phys. **0203** (2002), 014; Z. Fodor, S.D. Katz and K.K. Szabo, Phys. Lett. B **568** (2003), 73.
- 7) C. R. Allton et al., Phys. Rev. D **66** (2002), 074507, Phys. Rev. D **68** (2003), 014507;
- 8) C. R. Allton et al., Phys. Rev. D **71** (2005), 054508.
- 9) S. Ejiri et al., [arXiv: hep-lat/0609075].
- 10) E. Laermann and O. Philipsen, Ann. Rev. Nucl. Part. Sci. **53** (2003), 163.
- 11) P. de Forcrand and O. Philipsen, Nucl. Phys. B **642** (2002), 290; Nucl. Phys. B **673** (2003), 170.
- 12) M. D’Elia and M.P. Lombardo, Phys. Rev. D **67** (2003), 014505; Phys. Rev. D **70** (2004), 074509.
- 13) R.D. Pisarski, Phys. Rev. D **62** (2000), 111501(R).
- 14) Y. Nambu and G. Jona-Lasinio, Phys. Rev. **122** (1961), 345; **124** (1961), 246.
- 15) U. Vogl and W. Weise, Prog. Part. Nucl. Phys. **27** (1991), 195; T. Hatsuda and T. Kunihiro, Phys. Reports **247** (1994), 221.
- 16) P.N. Meisinger and M.C. Ogilvie, Nucl. Phys. Proc. Suppl. **47** (1996), 519; Phys. Lett. B **379** (1996), 163.
- 17) K. Fukushima, Phys. Lett. B **553** (2003), 38; Phys. Rev. D **68** (2003), 045004.
- 18) K. Fukushima, Phys. Lett. B **591** (2004), 277; Y. Hatta and K. Fukushima, Phys. Rev. D **69** (2004), 097502.
- 19) C. Ratti, M. A. Thaler and W. Weise, Phys. Rev. D **73** (2006), 014019.
- 20) C. Ratti, S. Rössner, M. A. Thaler and W. Weise, Eur. Phys. J. C **49** (2007), 213.
- 21) S. Rössner, C. Ratti and W. Weise, Phys. Rev. D **75** (2007), 034007.
- 22) C. Ratti, S. Rössner and W. Weise, Phys. Lett. B **649** (2007), 57.

- 23) W. Weise, C. Ratti and S. Rössner, Prog. Theor. Phys. Suppl. No. 168 (2007), 435.
- 24) S.K. Ghosh, T.K. Mukherjee, M.G. Mustafa and R. Ray, Phys. Rev. D **73** (2006), 114007.
- 25) E. Megias, E. Ruiz Arriola and L.L. Salcedo, Phys. Rev. D **74** (2006), 065005,114014.
- 26) C. Sasaki, B. Friman and K. Redlich, [arXiv:hep-ph/0611147].
- 27) G. Boyd *et al.*, Nucl. Phys. B **469** (1996), 419.
- 28) K. Fukushima, arXiv:0803.3318 [hep-ph].
- 29) F. Karsch, F. Laermann and A. Peikert, Nucl. Phys. B **605** (2001), 597.
- 30) F. Karsch *et al.*, arXiv:0804.4148 [hep-lat].
- 31) S. Rössner, T. Hell, C. Ratti and W. Weise, *The chiral and deconfinement crossover transitions: PNJL model beyond mean field*, arXiv:0712.3152 [hep-ph].
- 32) C. Bernard *et al.*, Phys. Rev. D **75** (2007), 094505.
- 33) N. Bratovic, diploma thesis, TU Munich (2008); N. Bratovic, T. Hell, S. Rössner and W. Weise, work in progress.
- 34) N. Yamamoto, M. Tachibana, T. Hatsuda and G. Baym, Phys. Rev. D **776** (2007), 074001.
- 35) P. de Forcrand, S. Kim and O. Philipsen, PoS Lat2007:178,2007; arXiv:0711.0262 [hep-lat].
- 36) T. Hell, S. Rössner, M. Cristoforetti and W. Weise, *Dynamics and thermodynamics of a non-local PNJL model*, in preparation (2008).
- 37) S. Fritsch, N. Kaiser and W. Weise Nucl. Phys. A **750** (2005), 259.
- 38) P. Finelli, N. Kaiser, D. Vretenar and W. Weise Nucl. Phys. A **770** (2006), 1.
- 39) N. Kaiser, P. de Homont and W. Weise Phys. Rev. C **77** (2008), 025204.
- 40) N. Kaiser and W. Weise, preprint (2008).